High Selectivity Balanced Filters Based on Transversal Signal-interaction Concepts

Wenjie Feng, Meiling Hong, and Wenquan Che

Department of Communication Engineering
Nanjing University of Science and Technology, Nanjing, 210094, China
fengwenjie1985@163.com

Abstract ─ Two novel high selectivity balanced filters based on transversal signal-interaction concepts with wideband common mode suppression are proposed in this paper. Four and six transmission zeros near each passband are realized to improve the selectivity for the differential mode. In addition, the common mode can be suppressed with insertion loss greater than 15 dB over a wide frequency band. Two prototypes ($\varepsilon_r = 2.65$, $h = 0.5$ mm, $\tan\delta = 0.003$) with 3-dB fractional bandwidths of 31.3% and 32% for the differential mode with upper stopband greater than 18 dB are designed and fabricated. Good agreements can be observed between measured results and theoretical expectations.

Index Terms ─ Balanced filter, differential/common mode, open/shorted coupled lines, transmission zeros, transversal signal-interaction concepts.

I. INTRODUCTION

Balanced circuits have recently attracted special attention in communication systems for their higher immunity to the environmental noises, better dynamic range, and lower electromagnetic interference [1]. Many different balanced filters with selective filtering of differential mode (DM) signal and suppression for common-mode (CM) response are illustrated in [2]-[12]. In [2], the multi-stage branch-line topologies on a single-layer microstrip line were utilized to design a class of wideband balanced filters, but these filters have disadvantages of large overall circuit area. Some differential ultra-wideband (UWB) balanced bandpass filters based on double-sided parallel-strip line (DSPSL) are illustrated in [3], however, the upper stopbands for the differential mode are a little narrow. In [4], wideband differential filters employing the transversal signal-interaction concept are used to improve the common mode suppression, as well as the simple design theory with large insertion loss. In [5], the low-loss balanced filter with wideband common mode suppression using microstrip-slotline coupling are realized, but the numbers of transmission zeros near the differential mode passband are difficult to increase. In addition, the T-shaped resonator in [6] and ring resonator in [7]-[8] were applied to design balanced filters. In [9], the common-mode suppression of the balanced bandpass filter can be kept at a high level by adding a varactor to the center of the resonator. In [10], a balanced SIW filter using source-load coupling is proposed. To further improve the selectivity of the balanced filters, coupled lines and quarter/half-wavelength open/shorted stubs have been widely used [11-12].

In this paper, two novel balanced filter circuits based on transversal signal-interaction concepts with multiple transmission zeros for the differential/common mode are proposed. Four and six transmission zeros near the differential mode passband can be easily realized using the transversal signal interference concept, and five and seven transmission zeros can be also used to realize wideband common mode suppression. Two prototypes of the balanced filters operating at 3.0 GHz are constructed on the dielectric substrate with $\varepsilon_r = 2.65$, $h = 0.5$ mm, and $\tan\delta = 0.003$.

II. ANALYSIS OF PROPOSED BALANCED FILTERS

In this section, two balanced filters based on transversal signal-interaction concepts are analyzed in detail. The differential mode and common mode circuit are used to analyze the transmission characteristics of the two balanced filters in *Part A* and *Part B*, the simulated results of the two balanced filters are given in *Part C*.

A. Balanced filter analysis (Structure I)

Figure 1 (a) shows the ideal circuit of the proposed balanced filter structure with four transmission zeros. Four open/shorted coupled lines (even/odd-mode characteristic impedance Z_{oe2} and Z_{oo2}, electrical length θ) with two quarter-wavelength transmission lines (characteristic impedance Z_1, electrical length θ) on each side are shunted connected in the input/output ports 1, 1', 2, 2'. Four open coupled lines (even/odd-mode characteristic impedance Z_{oe1} and Z_{oo1}, electrical length θ) are located in the center of the equivalent circuit with two shorted stubs (characteristic impedance Z_1, electrical

Submitted On: April 5, 2016
Accepted On: July 15, 2016

length θ) and an open stub (characteristic impedance Z_1, electrical length 2θ). The characteristic impedances of the microstrip lines at the input/output ports are $Z_0 = 50\ \Omega$.

When the differential mode signals are excited from ports 1 and 1' in Fig. 1 (a), a virtual short appears along the symmetric lines, as shown in Fig. 1 (b). The odd-mode equivalent circuits for the differential mode are shown in Fig. 2 (a), and the even/odd-mode input admittances for the differential mode are:

$$Y_{o1-DM} = -j\frac{2\cos\theta\left[2Z_{oe1}Z_{oo1}\cos^2\theta - Z_1(Z_{oe1}+Z_{oo1})\sin^2\theta\right]}{2Z_{oe1}Z_{oo1}(Z_{oe1}+Z_{oo1})\sin\theta\cos^2\theta + Z_1\sin\theta\left[(Z_{oe1}+Z_{oo1})^2\cos^2\theta - (Z_{oe1}-Z_{oo1})^2\right]} + j\frac{-(Y_{oe2}+Y_{oo2})^2 Z_2\cos^2\theta + (Y_{oo2}-Y_{oe2})^2 Z_2 + 2(Y_{oe2}+Y_{oo2})\sin^2\theta}{(Y_{oe2}+Y_{oo2})^2 Z_2^2\sin\theta\cos\theta - (Y_{oo2}-Y_{oe2})^2 Z_2^2\tan\theta + (Y_{oe2}+Y_{oo2})Z_2\sin 2\theta}, \quad (1)$$

$$Y_{e1-DM} = \frac{j[4Z_1\tan^2\theta - 2(Z_{oe1}+Z_{oo1})]}{(Z_{oe1}+Z_{oo1})(2Z_1+Z_{oe1}+Z_{oo1})\tan\theta} + \frac{j[Z_2(Z_{oe2}+Z_{oo2})+2Z_{oe2}Z_{oo2}]}{2Z_{oe2}Z_{oo2}\cot\theta - Z_2^2(Z_{oe2}+Z_{oo2})\tan\theta}, \quad (2)$$

$$Y_{o2-DM} = -j\frac{2\cos\theta\left[2Z_{oe1}Z_{oo1}\cos^2\theta - Z_1(Z_{oe1}+Z_{oo1})\sin^2\theta\right]}{2Z_{oe1}Z_{oo1}(Z_{oe1}+Z_{oo1})\sin\theta\cos^2\theta + Z_1\sin\theta\left[(Z_{oe1}+Z_{oo1})^2\cos^2\theta - (Z_{oe1}-Z_{oo1})^2\right]} + j\frac{Z_2(Z_{oe2}+Z_{oo2})+2Z_{oe2}Z_{oo2}}{2Z_2Z_{oe2}Z_{oo2}\cot\theta - Z_2^2(Z_{oe2}+Z_{oo2})\tan\theta}, \quad (3)$$

$$Y_{e2-DM} = Y_{e1-DM}. \quad (4)$$

When $Y_{e/o\text{-}DM}=0$, the resonator frequencies in the passband for the odd-mode for the differential mode can be calculated as:

$$\theta_{o1} = \arccos\sqrt{\frac{-B\pm\sqrt{B^2-4AC}}{2A}}, \quad \theta_{o2} = \pi - \arccos\sqrt{\frac{-B\pm\sqrt{B^2-4AC}}{2A}},$$
$$A = a_1^2 a_2 Z_1(a_2Z_2+2) + 2a_1a_2^2 Z_2(Z_1Z_2+Z_{oe1}Z_{oo1}) + 4a_1a_2(Z_1Z_2+Z_{oe1}Z_{oo1}) + 4a_2Z_2Z_{oe1}Z_{oo1}(a_2Z_2+2),$$
$$B = -[a_1^2 Z_1(b_2^2Z_2+2a_2) + 2a_1a_2(a_2Z_1Z_2^2 + 2Z_1Z_2 + 2Z_{oe1}Z_{oo1}) + 2a_1b_2^2Z_1Z_2^2 + 2a_1b_2^2Z_2Z_{oe1}Z_{oo1} + a_2b_1^2Z_1(a_2Z_2+2) + 4b_2^2Z_2^2Z_{oe1}Z_{oo1}],$$
$$C = 2a_1b_2^2Z_1Z_2^2 + b_1^2b_2^2Z_1Z_2 + 2a_2b_1^2Z_1,$$
$$a_1 = Z_{oe1}+Z_{oo1}, \quad b_1 = Z_{oe1}-Z_{oo1},$$
$$a_2 = Y_{oe2}+Y_{oo2}, \quad b_2 = Y_{oo2}-Y_{oe2}. \quad (5)$$

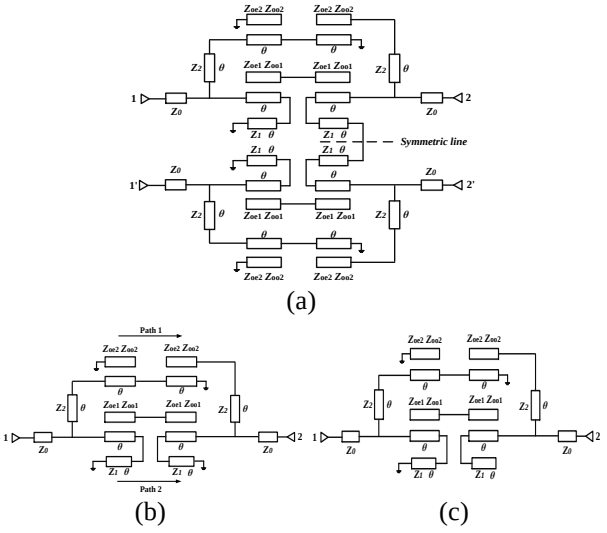

Fig. 1. (a) The ideal circuit of the balanced filter, (b) equivalent circuit for the differential mode, and (c) equivalent circuit for the common mode. (*Structure I*).

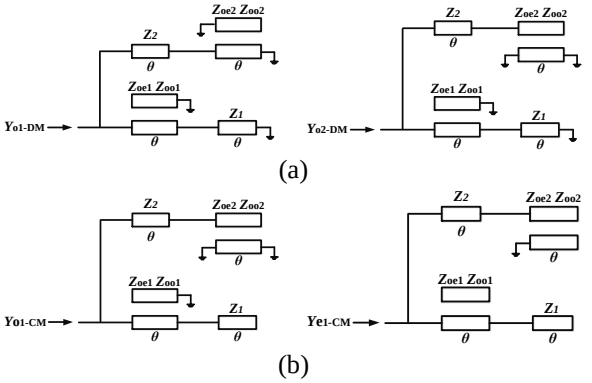

Fig. 2. (a) Odd-mode equivalent circuit of differential mode circuit, and (b) even/odd-mode equivalent circuit of common mode circuit. (*Structure I*).

Figures 3 (a)-(d) plot the odd-mode resonant frequencies versus θ and the simulated results of the circuit in Figs. 1 (b)-(c). Due to the superposition of signals for Paths 1 and 2, four transmission zeros (f_{tz1},

f_{tz2}, f_{tz3}, f_{tz4}) can be easily achieved for the proposed balanced filter [13]. The 3-dB bandwidth of the differential mode is mainly determined by the odd-modes f_{o1} and f_{o2}. In addition, the odd-modes f_{o1} and f_{o2} move towards f_0 as Z_1 increases, and the 3-dB bandwidth of the differential mode increases as the coupling coefficient k_1 ($k_1 = (Z_{oe1}-Z_{oo1})/(Z_{oe1}+Z_{oo1})$) increases. The unwanted even/odd modes for the common mode can be suppressed less than -30 dB by the five transmission zeros. Four transmission zeros (f_{tz1}, f_{tz2}, f_{tz3}, f_{tz4}) move away from f_0 as the characteristic impedance Z_1 increases. In this way, the out-of-band harmonic suppression of the differential mode can be adjusted by the characteristic impedance Z_2 without changing the bandwidth of the differential mode. Next, to further improve the selectivity and the common mode suppression of the balanced filter with four transmission zeros, another high selectivity balanced filter structure with six transmission zeros close to the differential mode passband, and wideband common mode suppression will be presented.

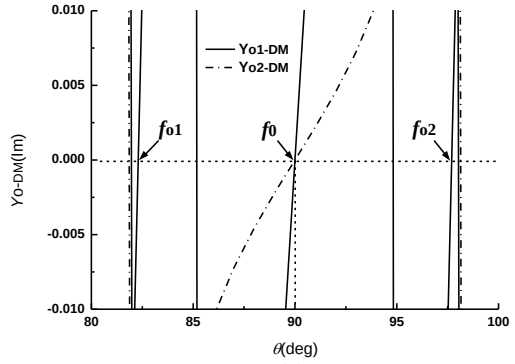

(a)

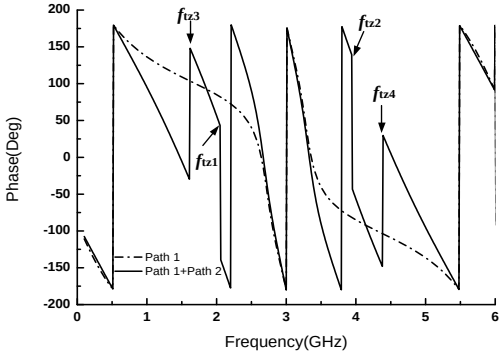

(b)

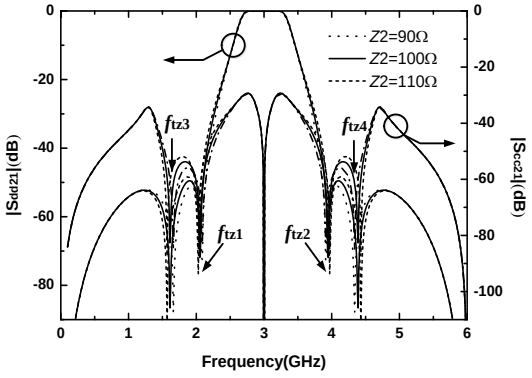

(c)

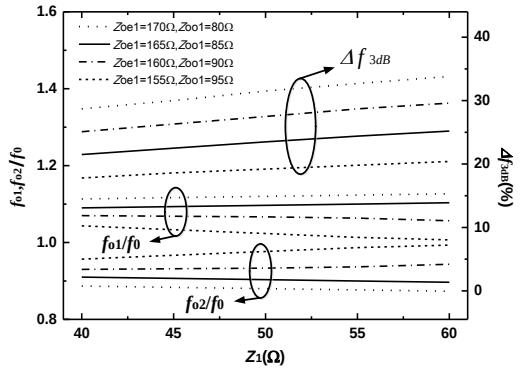

(d)

Fig. 3. (a) Analysis of resonator frequencies versus θ. (b) phase of $|S_{dd21}|$ (Z_0= 50 Ω, Z_1=50 Ω, Z_2=100 Ω, Z_{oe1} =160 Ω, Z_{oo1}=90 Ω, Z_{oe2} =150 Ω, Z_{oo2} =110 Ω, f_0= 3.0 GHz, θ= 90°). (c) $|S_{dd21}|$& $|S_{cc21}|$ versus Z_2. (d) f_{o1}, f_{o2}/f_0, Δf_{3dB} versus Z_{oe1}, Z_{oo1}, Z_1. (*Structure I*).

B. Balanced filter analysis (Structure II)

Figure 4 (a) shows the ideal circuit of the balanced filter structure with two half-wavelength open stubs (Z_3, 2θ), instead of two quarter-wavelength short stubs (Z_1, θ), and the other part is the same as the balanced filter of *Structure I*.

As discussed in *Part A*, when the differential/ common mode are excited from ports 1 and 1' in Fig. 4 (a), a virtual short/open appears along the symmetric lines. The even/odd-mode equivalent circuits for the differential/common mode are shown Figs. 5 (a)-(b), and the input admittance for the differential mode of Fig. 5 (a) can be illustrated as:

$$Y_{o1-DM} = j\frac{Z_3(Z_{oe1}+Z_{oo1})\sin 2\theta\cos 2\theta + 4Z_{oe1}Z_{oo1}\sin 2\theta\cos^2\theta}{Z_3\cos 2\theta\left[(Z_{oe1}-Z_{oo1})^2-(Z_{oe1}+Z_{oo1})^2\cos^2\theta\right]-Z_{oe1}Z_{oo1}(Z_{oe1}+Z_{oo1})\sin^2 2\theta} \tag{6}$$
$$+ j\frac{-(Y_{oe2}+Y_{oo2})^2 Z_2\cos^2\theta + (Y_{oo2}-Y_{oe2})^2 Z_2 + 2(Y_{oe2}+Y_{oo2})\sin^2\theta}{(Y_{oe2}+Y_{oo2})^2 Z_2^2\sin\theta\cos\theta-(Y_{oo2}-Y_{oe2})^2 Z_2^2\tan\theta+(Y_{oe2}+Y_{oo2})Z_2\sin 2\theta},$$

$$Y_{e1-DM} = \frac{-j[2(Z_{oe1}+Z_{oo1})\tan 2\theta + 4Z_3\tan\theta]}{(Z_{oe1}+Z_{oo1})^2\tan\theta\tan 2\theta - 2Z_3(Z_{oe1}+Z_{oo1})} \tag{7}$$
$$+\frac{j[Z_2(Z_{oe2}+Z_{oo2})+2Z_{oe2}Z_{oo2}]}{2Z_2Z_{oe2}Z_{oo2}\cot\theta - Z_2^2(Z_{oe2}+Z_{oo2})\tan\theta}.$$

When $Y_{e/o\text{-}DM}=0$, the resonator frequencies in the passband for the even -mode for the differential mode can be calculated as:

$$\theta_{e1}=\arctan\sqrt{\frac{-B\pm\sqrt{B^2-4AC}}{2A}},\quad \theta_{e2}=\pi-\arctan\sqrt{\frac{-B\pm\sqrt{B^2-4AC}}{2A}},$$

$$A=-4Z_1Z_2{}^2(Z_{oe1}+Z_{oo1}),$$

$$B=(Z_{oe1}+Z_{oo1})^2[2Z_{oe2}Z_{oo2}+Z_2(Z_{oe2}+Z_{oo2})]+2(Z_{oe1}+Z_{oo1})(Z_{oe2}+Z_{oo2})(Z_1Z_2+Z_2{}^2)$$
$$+4Z_1Z_{oe2}Z_{oo2}(Z_{oe1}+Z_{oo1})+8Z_1Z_2Z_{oe2}Z_{oo2},$$

$$C=-4Z_2Z_{oe2}Z_{oo2}(Z_{oe1}+Z_{oo1}). \quad (8)$$

Figures 6 (a)-(c) show the even/odd-mode resonant frequencies for the differential mode circuit versus θ and the simulated results of the circuit in Figs. 4 (b)-(c). Due to the superposition of signals for Paths 1 and 2, six transmission zeros (f_{tz1}, f_{tz2}, f_{tz3}, f_{tz4}, f_{tz5}, f_{tz6}) can be easily achieved for the proposed balanced filter [13]. Compared with the balanced filter of *Structure I*, two additional transmission zeros (f_{tz5}, f_{tz6}) are located at $0.5f_0$ and $1.5f_0$, which can be used to further improve the differential mode passband selectivity and the common mode suppression level from 0 to f_{tz1}, f_{tz2} to $2\,f_0$. In addition, the locations of two transmission zeros (f_{tz5}, f_{tz6}) do not change with all parameters of the circuit, and the locations of another four transmission zeros (f_{tz1}, f_{tz2}, f_{tz3}, f_{tz4}) do not change with Z_{oe1}, Z_{oo1}, Z_1 and Z_3. The 3-dB bandwidth of the differential mode is mainly determined by the even-modes f_{e1} and f_{e2}, and the 3-dB bandwidth of the differential mode decreases and differential/common mode suppression becomes better with the decrease of k_1 (k_1= (Z_{oe1}-Z_{oo1})/(Z_{oe1}+Z_{oo1})). The common mode can be suppressed less than -30 dB by the seven transmission zeros. Compared with the balanced filter of *Structure I*, the selectivity and common mode suppression of the balanced filter of *Structure II* has been further improved.

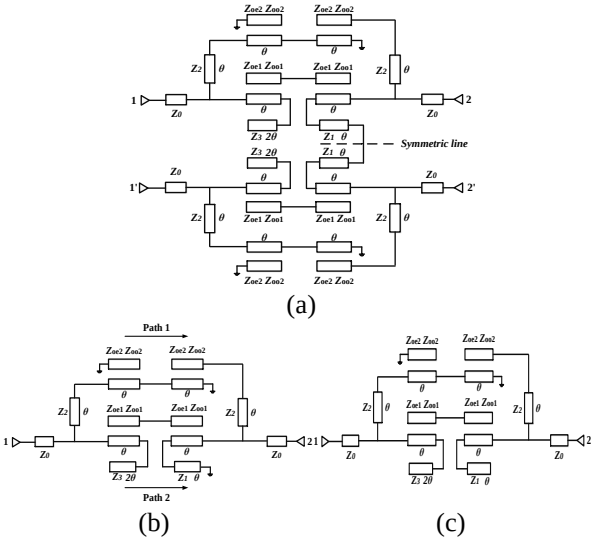

Fig. 4. (a) The ideal circuit of the balanced filter, (b) equivalent circuit for the differential mode, and (c) equivalent circuit for the common mode. (*Structure II*).

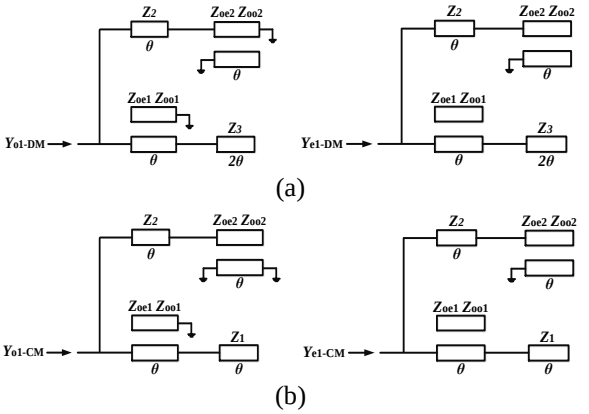

Fig. 5 (a) Even/odd-mode equivalent circuit of differential mode circuit, and (b) even/odd-mode equivalent circuit of common mode circuit. (*Structure II*).

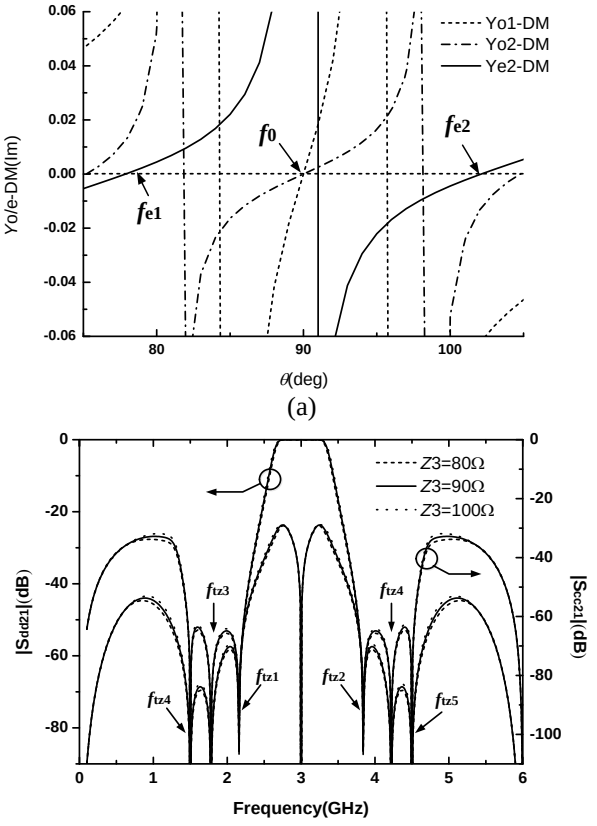

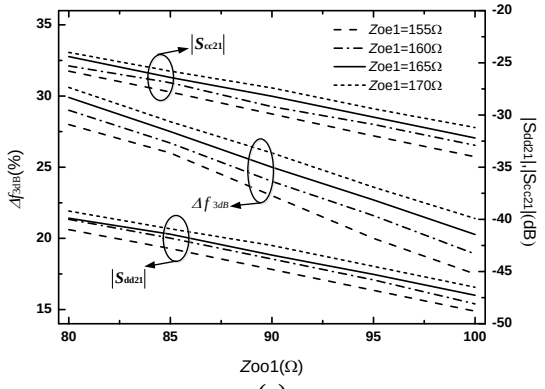

(c)

Fig. 6. (a) Analysis of resonator frequencies versus θ for the differential mode. (b) $|S_{dd21}|$& $|S_{cc21}|$ versus Z_3 (Z_0 = 50 Ω, Z_1 =50 Ω, Z_2 =70 Ω, Z_{oe1} =160 Ω, Z_{oo1} =90 Ω, Z_{oe2} =150 Ω, Z_{oo2} =110 Ω, f_0 = 3.0 GHz, θ= 90°). (c) Δf_{3dB}, $|S_{dd21}|$, $|S_{cc21}|$ versus Z_{oe1}, Z_{oo1}. (*Structure II*).

C. Proposed two balanced bandpass filters

Referring to the discussions and the simulated results in *Part A and B*, the final parameters for the filters of Figs. 1, 4 are listed as below: Z_0 = 50 Ω, Z_1 = 50 Ω, Z_2 = 100 Ω, Z_{oe1}= 160 Ω, Z_{oo1} = 90 Ω, Z_{oe2} = 150 Ω, Z_{oo1} = 110 Ω; Z_0 = 50 Ω, Z_1 = 50 Ω, Z_2 = 70 Ω, Z_3 = 90 Ω, Z_{oe1} = 160 Ω, Z_{oo1} =90 Ω, Z_{oe2} =150 Ω, Z_{oo1} =110 Ω. The structure parameters for two balanced filters (52.28 mm × 35.85 mm, 55.48 mm × 36.26 mm) shown in Figs. 7 (a)-(b) are: l_1 = 15.31 mm, l_2 = 17.5 mm, l_3 = 6.66 mm, l_4 = 10.42 mm, l_5 = 15.46 mm, l_6 = 16.06 mm, l_7 = 10.6 mm, l_8 = 12.55 mm, l_9 = 11.65 mm, l_{10} = 4.2 mm, l_{11} = 9.42 mm, l_{12} = 4 mm, w_0 = w_3= w_5 =1.34 mm, w_1 = 0.2 mm, w_2 = 0.35 mm, w_4 = 0.3 mm, s_1 = s_2 = 0.2 mm, t_1 =t_2 = 1.89 mm, d = 0.7 mm; l_1 = 15.79 mm, l_2 = 17.5 mm, l_3 = 4.55 mm, l_4 = 10.42 mm, l_5 = 4 mm, l_6 = 18 mm, l_7 = 16.96 mm, l_8 = 17.56 mm, l_9 = 12.3 mm, l_{10} = 8.75 mm, l_{11} = 13.76 mm, l_{12} = 4.3 mm, l_{13} = 9.32 mm, l_{14} = 4 mm, w_0 = w_5 = 1.34 mm, w_1 = 0.2mm, w_2 = 0.76 mm, w_3 = 0.45 mm, w_4 = 0.3 mm, s_1 = s_2 = 0.2 mm, t_1 = t_2 = 1.89 mm, d = 0.7 mm.

Figures 8-9 illustrate the simulated results of the two balanced filters with four/six transmission zeros (Simulated with ANSYS HFSS v.13.0). For the differential mode of balanced filter of *Structure I*, four simulated transmission zeros are located at 1.52, 2.23, 3.88 and 4.64 GHz, the in-band insertion loss is less than 0.5 dB with 3-dB bandwidth approximately 30.7% (2.54-3.46 GHz); for the common mode, the insertion loss is greater than 17 dB from 0 GHz to 8.5 GHz, indicating good wideband rejection. Moreover, for the differential mode of the balanced filter of *Structure II*, five simulated transmission zeros are located at 1.44, 2.29, 3.63, 4.1 and 4.87 GHz, the 3-dB bandwidth is 29% (2.44-3.31 GHz) with return loss greater than 13 dB (2.56-3.34 GHz); for the common mode, over 15-dB common mode suppression is achieved from 0 GHz to 8.92 GHz.

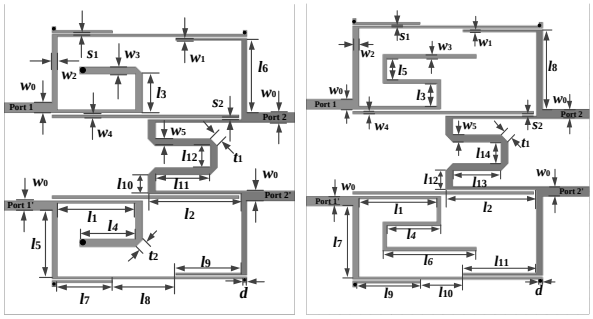

(a) (b)

Fig. 7. Geometries of two proposed balanced filters: (a) *Structure I*, and (b) *Structure II*.

III. MEASURED RESULTS AND DISCUSSIONS

For comparisons, the measured *S*-parameters of the two balanced filters are also illustrated in Figs. 8-9. For the differential mode of the balanced filter of *Structure I*, the 3-dB bandwidth is 31.3% (2.57-3.51 GHz) with return loss greater than 13 dB, four measured transmission zeros are located at 1.03, 2.32, 3.9 and 4.63 GHz, the insertion loss in the passband is less than 0.6 dB and greater than 20 dB from 3.75 to 8.9 GHz (2.97f_0); for the common mode, the insertion loss is greater than 15 dB from 0 GHz to 8.8 GHz (2.93f_0). For the differential mode of the balanced filter of *Structure II*, six measured transmission zeros are located at 1.21, 1.61, 2.26, 3.72, 4.14 and 4.96 GHz with 3-dB bandwidth of 32% (2.48-3.44 GHz), the insertion loss is less than 0.7 dB with return loss greater than 10 dB from 2.4 GHz and 3.53 GHz, an upper stopband with insertion loss greater than 20 dB is realized from 3.59 to 8.94 GHz (2.98f_0); in addition, the insertion loss for the common mode is greater than 15 dB from 0 to 9 GHz (3f_0). The slight frequency discrepancies of measured passbands for the differential mode are mainly caused by the imperfect soldering skill of the shorted stubs and folded transmission line of the two balanced filters.

To further illustrate the characteristics of the two balanced filters, Table 1 illustrates the comparisons of measured results for several balanced filter structures. Compared with other balanced filters [3]-[12], more transmission zeros near the passband are obtained for the two balanced filter structures, and the upper stopbands for the differential mode of the two balanced filters stretch up to 2.97f_0 ($|S_{dd21}|$<-20 dB) and 2.98f_0 ($|S_{dd21}|$<-20 dB). The insertion losses are lower with 0.6 dB and 0.7 dB for the proposed balanced filters.

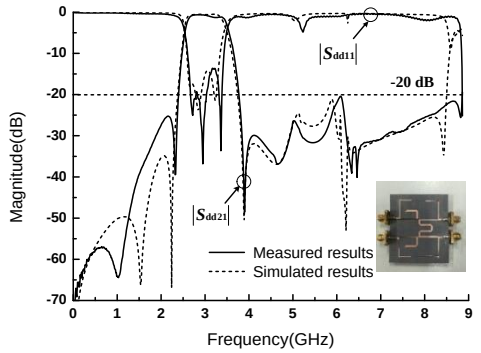

(a)

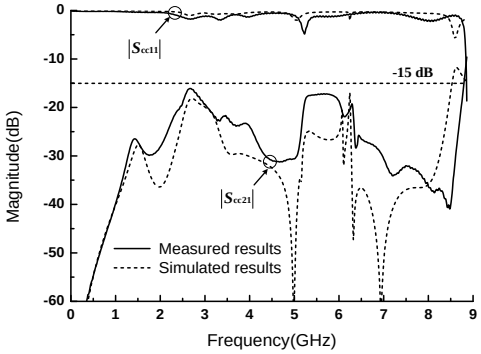

(b)

Fig. 8. Photograph, measured and simulated results of *Structure I*: (a) differential mode and (b) common mode.

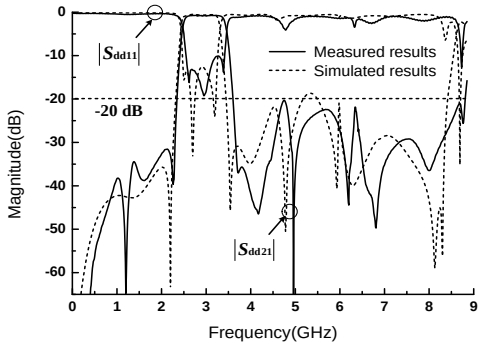

(a)

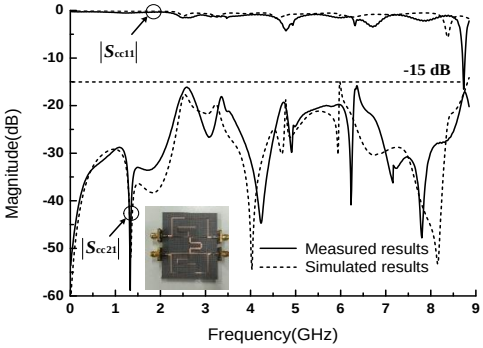

(b)

Fig. 9. Photograph, measured and simulated results of *Structure II*: (a) differential mode and (b) common mode.

Table 1: Comparisons of measured results for some balanced filters

Filter Structures	TZs, $\|S_{dd21}\|$ 0-2f_0, (f_0)	FBW $\|S_{dd21}\|$	Stopband $\|S_{dd21}\|$, dB	$\|S_{cc21}\|$, dB
Ref. [3]	0 (3.0 GHz)	110%	<-20, 2.2 f_0	<-15, (0-8)
Ref. [6] - II	2 (6.85 GHz)	70.7%	<-20, 2.77 f_0	<-13.5, (0-19.5)
Ref. [8]	4 (2.4 GHz)	17%	<-15, 2.75 f_0	<-18.8, (0-6.5)
Ref. [11] - I	3 (5.0 GHz)	67.6%	<-15, 2.7 f_0	<-15, (1.9-8.3)
Ref. [11] - II	5 (5.0 GHz)	37.8%	<-15,2.8 f_0	<-20, (1.2-9.3)
Ref. [12]	3 (3.0 GHz)	82%	<-15,2.1 f_0	<-10, (1.65-3.95)
Structure I	4 (3.0 GHz)	31.3%	<-20, 2.97f0	<-15, (0-8.8)
Structure II	6 (3.0 GHz)	32.0%	<-20, 2.98f0	<-15, (0-9)

IV. CONCLUSION

In this paper, two novel balanced filters based on transversal signal-interaction concepts with multiple transmission zeros are proposed. Four and six transmission zeros close to the differential mode passband can be easily achieved using the transversal signal-interaction concepts. In addition, wideband common mode suppression can easily realized by the multiple transmission zeros. High selectivity and wideband common mode suppression are obtained for the two balanced filters, indicating good candidates for microwave wireless applications.

ACKNOWLEDGMENT

This work is supported by the 2012 Distinguished Young Scientist awarded by the National Natural Science Foundation Committee of China (61225001), and by National Natural Science Foundation of China (6140010914), Natural Science Foundation of Jiangsu Province (BK20140791) and the 2014 Zijin Intelligent Program of Nanjing University of Science and Technology.

REFERENCES

[1] F. Broydé and E. Clavelier, "Crosstalk in balanced interconnections used for differential signal transmission," *IEEE Trans. Circuits Syst. I, Reg. Papers*, vol. 54, no. 7, pp. 1562-1572, July 2007.

[2] T. B. Lim and L. Zhu, "A differential-mode wideband bandpass filter on microstrip line for UWB application," *IEEE Microw. Wirel. Compon. Lett.*, vol. 19, no. 10, pp. 632-634, Oct. 2009.

[3] X. H. Wang, Q. Xue, and W. W. Choi, "A novel ultra-wideband differential filter based on double-sided parallel-strip line," *IEEE Microw. Wireless Compon. Lett.*, vol. 20, no. 8, pp. 471-473, Oct. 2010.

[4] H. T. Zhu, W. J. Feng, W. Q. Che, and Q. Xue, "Ultra-wideband differential bandpass filter based on transversal signal-interference concept," *Electron. Lett.*, vol. 47, no. 18, pp. 1033-1035, Sep. 2011.

[5] J. Shi, C. Shao, J. X. Chen, Q. Y. Lu, Y. J. Peng, and Z. H. Bao, "Compact low-loss wideband differential bandpass filter with high common mode suppression," *IEEE Microw. Wireless Compon. Lett.*, vol. 23, no. 9, pp. 480-482, Sep. 2013.

[6] W. J. Feng and W. Q. Che, "Novel wideband differential bandpass filters based on T-shaped structure," *IEEE Trans. Microw. Theory Tech.*, vol. 60, no. 6, pp. 1560-1568, June 2012.

[7] W. J. Feng, W. Q. Che, and Q. Xue, "Balanced filters with wideband common mode suppression using dual-mode ring resonators," *IEEE Trans. Circuits Syst. I*, vol. 62, no. 6, pp. 1499-1507, June 2015.

[8] L. L. Qiu and Q. X. Chu, "Balanced bandpass filter using stub-loaded ring resonator and loaded coupled feed-line," *IEEE Microw. Wireless Compon. Lett.*, vol. 25, no. 10, pp. 654-656, Oct. 2015.

[9] Q. Y. Lu, J.-X. Chen, L.-H. Zhou, and H. Tang, "Novel varactor-tuned balanced bandpass filter with continuously high common-mode suppression," *ACES Jour.*, vol. 28, no. 7, pp. 628-632, July 2013.

[10] Q. Xiao, C. X. Zhou, "Design of balanced SIW filter with transmission zeroes and linear phase," *ACES Jour.*, vol. 30, no. 9, pp. 1019-1023, Sep. 2015.

[11] W. J. Feng, X. Gao, W. Q. Che, W. C. Yang, and Q. Xue, "High selectivity wideband balanced filters with multiple transmission zeros," *IEEE Trans. Circuits Syst. II*, vol. PP, no. 99, pp. 1-1, May 2015.

[12] X. H. Wang, S. Hu, and Q. Y. Cao, "Differential broadband filter based on microstrip coupled line structures," *Electron. Lett.*, vol. 50, no. 15, pp. 1069-1070, July 2014.

[13] W. J. Feng, W. Q. Che, and Q. Xue, "Transversal signal interaction: Overview of high-performance wideband bandpass filters," *IEEE Microw. Magazine*, vol. 15, no. 2, pp. 84-96, Mar. 2014.

Wenjie Feng was born in Shangqiu, Henan Province, China, in 1985. He received the B.Sc. degree from the First Aeronautic College of the Airforce, Xinyang, China, in 2008, the M.Sc. and Ph.D. degrees from the Nanjing University of Science and Technology (NUST), Nanjing, China, in 2010, 2013.

From November 2009 to February 2010, March 2013 to September 2013, he was a Research Assistant with the City University of Hong Kong. From October 2010 to March 2011, he was an exchange student with the Institute of High-Frequency Engineering, Technische Universität München, Munich, Germany. He is currently an Associate Professor with the Nanjing University of Science and Technology, Nanjing, China. He has authored or co-authored over 110 internationally referred journal and conference papers. He has obtained the second class science and technology award and best dissertation award of Jiangsu Province in 2015. His research interests include ultra-wideband (UWB) circuits and technologies, substrate integrated components and systems, planar microstrip filters and power dividers, LTCC circuits.

Feng is a Reviewer for over twenty internationally referred journal and conference papers, including ten IEEE Transactions and three IEEE Letters. He now serves as an Associate Editor for the *International Journal of Electronics.*

Meiling Hong was born in Nantong, Jiangsu Province, China, in 1991. She received the B.E. degree from the Nanjing University of Science and Technology (NUST), Nanjing, China, in 2014. From September 2014, she went to Nanjing University of Science and Technology (NUST), Nanjing, China, for further study as a postgraduate. Her research interests include passive device and circuit.

Wenquan Che received the B.Sc. degree from the East China Institute of Science and Technology, Nanjing, China, in 1990, the M.Sc. degree from the Nanjing University of Science and Technology (NUST), Nanjing, China, in 1995, and the Ph.D. degree from the City University of Hong Kong (CITYU), Kowloon, Hong Kong, in 2003.

In 1999, she was a Research Assistant with the City University of Hong Kong. From March 2002 to September 2002, she was a Visiting Scholar with the Polytechnique de Montréal, Montréal, QC, Canada. She is currently a Professor with the Nanjing University of Science and Technology, Nanjing, China. From 2007 to 2008, she conducted academic research with the Institute of High Frequency Technology, Technische Universität München. During the summers of 2005–2006 and 2009–2012, she was with the City University of Hog Kong, as Research Fellow and Visiting Professor. She has authored or co-authored over 200 internationally referred journal papers and international conference papers. She has been a Reviewer for *IET Microwaves, Antennas and Propagation*. Her research interests include electro-

magnetic computation, planar/coplanar circuits and subsystems in RF/microwave frequency, microwave monolithic integrated circuits (MMICs) and medical application of microwave technology.

Che is a Reviewer for the IEEE Transactions on Microwave Theory and Techniques, IEEE Transactions on Antennas and Propagation, IEEE Transactions on Industrial Electronics, and IEEE Microwave and Wireless Components Letters. She was the recipient of the 2007 Humboldt Research Fellowship presented by the Alexander von Humboldt Foundation of Germany, the 5th China Young Female Scientists Award in 2008 and the recipient of Distinguished Young Scientist awarded by the National Natural Science Foundation Committee (NSFC) of China in 2012.